Bulletin of Mathematical Biology (2009) 71: 952–979
DOI 10.1007/s11538-008-9389-z

ORIGINAL ARTICLE

Modeling the Evolution of Insect Phenology

Brian P. Yurk*, James A. Powell

Department of Mathematics and Statistics, Utah State University, Logan, UT 84322-3900, USA

Received: 31 May 2008 / Accepted: 5 December 2008 / Published online: 20 December 2008

Abstract Climate change is likely to disrupt the timing of developmental events (phenology) in insect populations in which development time is largely determined by temperature. Shifting phenology puts insects at risk of being exposed to seasonal weather extremes during sensitive life stages and losing synchrony with biotic resources. Additionally, warming may result in loss of developmental synchronization within a population making it difficult to find mates or mount mass attacks against well-defended resources at low population densities. It is unknown whether genetic evolution of development time can occur rapidly enough to moderate these effects. We present a novel approach to modeling the evolution of phenology by allowing the parameters of a phenology model to evolve in response to selection on emergence time and density. We use the Laplace method to find asymptotic approximations for the temporal variation in mean phenotype and phenotypic variance arising in the evolution model that are used to characterize invariant distributions of the model under periodic temperatures at leading order. At these steady distributions the mean phenotype allows for parents and offspring to be oviposited at the same time of year in consecutive years. Numerical simulations show that populations evolve to these steady distributions under periodic temperatures. We consider an example of how the evolution model predicts populations will evolve in response to warming temperatures and shifting resource phenology.

Keywords Phenology · Evolution · Mathematical model · Quantitative genetics · Laplace method · Climate change · Indirect selection

1. Introduction

Can evolution moderate the disruptive effects of global warming on phenology, the timing of developmental milestones such as emergence or oviposition, in insect populations? There are strong selective pressures on insects to maintain appropriate phenology, including developmental synchrony with resources and within populations. Insect phenology changes as yearly temperature changes, because the time necessary for an

*Corresponding author.
E-mail address: brian.yurk@aggiemail.usu.edu (Brian P. Yurk).

insect to complete its life cycle is largely dependent on temperature (Zaslavski, 1988). This link has been observed in populations around the globe; recent temperature change has been linked to shifting phenology (Parmesan and Yohe, 2003) and range expansion (Carroll et al., 2003) in multiple populations. It is not well understood how evolution of temperature-dependent development time may moderate the effects of increasing temperature on phenology. In this paper, we present a novel approach to modeling the evolution of temperature-dependent development time in response to selection on phenology.

An individual's phenology relative to the timing of abiotic factors and the phenology of other organisms has a major effect on its fitness. It is essential that development is timed to avoid the coincidence of sensitive life stages with extreme weather to lessen the risk of desiccation in the summer or cold-induced mortality in the winter (Logan and Powell, 2001). An individual's fitness may also be highly dependent on synchrony between its phenology and the phenology of its biotic resources. This is apparent in plant-pollinator systems, where the timing of pollinator flight activity must coincide with the timing of flower production (Memmott et al., 2007), and in plant-herbivore systems, where the timing of certain developmental stages must coincide with resource availability. For example, winter moth (*Operophtera brumata*) fitness is highly dependent on the coincidence of egg hatching with oak (*Quercus robur*) bud break (Visser and Holleman, 2001).

Developmental synchrony within a population can also be an important determinant of fitness, especially at low population densities. Finding mates can be difficult when there are few individuals within a population with overlapping reproductive periods (Calabrese and Fagan, 2004). Developmental synchrony within a population of herbivorous insects may also be a necessity at low population densities to overwhelm resource defenses. For example, mountain pine beetles (*Dendroctonus ponderosae* Hopkins) have short periods of flight activity during which they must attack pine trees in large enough numbers to result in tree mortality (Berryman et al., 1985). Both the need for reproductive synchrony, and the need for developmental synchrony for mass attack result in an Allee effect, in which the fitness of an emerging individual at low population densities increases with the emergence density (Allee et al., 1949). However, interspecific competition for resources becomes the dominant effect at high emergence densities, and increasing emergence density reduces fitness.

Temperature plays a major role in determining the phenology (and hence the fitness) of poikilothermic organisms such as insects. The body temperature of poikilotherms is not internally regulated; instead, their body temperature, and consequently their metabolic rate depend on ambient temperature, causing them to develop at different rates at different temperatures (Sharpe and DeMichele, 1977; Eubank et al., 1973). At low to moderate temperatures increasing temperature speeds metabolism resulting in a shorter time period required for development. At high temperatures, however, increasing temperature can be counterproductive, resulting in longer development time (Bentz et al., 1991). We make the distinction between development time, the time it takes for an insect to develop through a life stage or life cycle, and phenology, the timing (i.e., time of year) of developmental milestones. Many insects possess physiological mechanisms using cues other than temperature to control phenology, such as diapause or photoperiod sensitivity (Zaslavski, 1988). However, for some insects phenology is directly controlled by the dependence of development time on temperature (Danks, 1987). For these insects, the response of phenology to temperature is a highly plastic trait, i.e., phenology can change in response to yearly temperature change with no underlying molecular evolution.

Previous phenology models describe the plastic response of phenology to temperature for systems in which phenology is under direct temperature control (e.g., Danks, 1987). This response is particularly well understood for mountain pine beetle. Although presented in a general context, our evolution model is based on generalizing models of mountain pine beetle phenology (see, for example, Jenkins et al., 2001). These models, described in detail in Section 2.1, predict that developmental synchrony within a population can only be maintained within a narrow range of mean annual temperatures; this range spans approximately 2.5°C for mountain pine beetle, and a 2°C increase in mean annual temperature (well within current estimates of climate warming within the mountain pine beetle range (Christensen et al., 2007)) would push temperatures outside of this range (Logan and Powell, 2001). In addition to losing developmental synchrony outside of this range of temperatures, populations that do not evolve cease to be strictly univoltine (one generation per year), which is likely to result in maladaptive developmental timing relative to weather extremes (Logan and Powell, 2001). On the other hand, even if temperatures do allow developmental synchrony within the population, there is no guarantee that the timing of developmental events will be adaptive. For example, over the 2.5°C range that the mountain pine beetle is predicted to maintain developmental synchrony its emergence time is predicted to advance by 60 days (Logan and Powell, 2001). It is unlikely that such a large degree of phenology advancement could be adaptive, especially if it occurs in a population in which fitness is highly dependent on synchronization with the phenology of a biotic resource.

Genetic evolution may allow insect phenology to adapt to changing selective pressures as temperatures increase. In order for natural selection to cause evolution of a trait within a population, there must be heritable variation in that trait within the population (Hartl, 2000). Variability in the dependence of development time on temperature has been observed in the mountain pine beetle both within a single population (Gilbert et al., 2004) and between distinct populations that are adapted to different local environments (Bentz et al., 2001). Laboratory experiments have shown this variability to be heritable (Bentz et al., 2001). The same study revealed a similar pattern of variation in body size between populations; it is likely that smaller insects complete development faster than larger insects under the same environmental conditions. In the future, body size may provide a more easily measured surrogate for development time. An interesting consequence of variability in development time is the potential for reproductive isolation within a population. In particular, insects with short development times will emerge before insects with long development times, and since reproduction occurs after emergence, individuals with similar phenotypes may be more likely to mate than individuals with very different phenotypes.

The dependence of insect development time on temperature varies continuously within a population. It is affected by many aspects of physiology and environment and is likely influenced by many genes. Hence, it is best regarded as a quantitative (multifactorial) trait (Kimura, 1965; Lande, 1975), as opposed to a discrete trait that is controlled by few genes and varies in a discrete manner. Quantitative genetic models describe how selection affects variation in quantitative traits and how that variation is inherited by successive generations (Slatkin, 1979; Johnoson and Barton, 2005; Slatkin, 1970). Typically some assumption is made about the shape of the phenotype distribution within a population (e.g., normality (Kimura, 1965)), and the quantitative genetic model describes how selection and reproduction affects the mean and variance of

the phenotype distribution for the next generation (Slatkin, 1970). We are unaware of any published quantitative genetic model that explicitly describes the evolution of phenology.

In this paper, we develop and analyze a general mathematical model of the evolution of phenology that is under direct temperature control. Variation in development time is accounted for by a parameter that scales temperature-dependent development time curves, and a well-established phenology model (Powell et al., 2000) is used to describe the effect of this variation on phenology (emergence time) within a population (Sections 2.1–2.3). We then model natural selection on emergence time and emergence density with an Allee effect (Section 2.4). These selection pressures indirectly affect the variation in the dependence of development time on temperature (i.e., an individual's phenotype). Inheritance of this variation through sexual reproduction is represented by assuming that offspring inherit the mean parent phenotype plus some small random deviation (Section 2.5). Our evolution model is made up of phenotype-dependent development, selection, and reproduction mappings composed. We characterize this seemingly complex map by its effect on a few simple population characteristics: the density, mean phenotype, and phenotypic variance of insects that are oviposited at each time of year (Section 2.6). We use this characterization to find an asymptotic approximation for the evolution model using Laplace's method (Section 3.1), which is employed to demonstrate the existence of steady phenotype distributions. These distributions have means approximately equal to the phenotypes that allow for parents and offspring to be oviposited at the same time of year and predictable variances (Section 3.2). Finally, we numerically validate the approximation results and demonstrate other dynamics of the evolution map for a model insect whose phenology is qualitatively similar to a large class of insect species (Sections 4.1–4.3).

2. Model development

2.1. Temperature dependent phenology model

The temperature-dependent phenology model that forms the foundation of our evolution model was originally developed to predict mountain pine beetle phenology (Powell et al., 2000), but is easily adapted to describe any insect whose development time depends directly on temperature. For such insects, let $\rho_i(T)$ be the time required for an individual to complete development through its ith life stage at constant temperature T. These development time curves are typically U-shaped (Taylor, 1981). Development time is minimized at some optimal temperature (often approximately 20°C) and increases as temperature get cooler or warmer (Sharpe and DeMichele, 1977). In practice, $\rho_i(T)$ is approximated by measuring development time at constant temperatures in a laboratory, then fitting an appropriate curve to the data (Bentz et al., 1991). A piecewise exponential curve captures the U-shaped dependence of development time on temperature:

$$\rho_i(T) = \begin{cases} a + \exp[b - cT], & T < \theta, \\ a + \exp[b - \theta(d + c) + dT], & T \geq \theta. \end{cases} \tag{1}$$

To maintain the appropriate U-shape and to avoid zero and negative development times, the parameters a, c, d are positive. An example of a development time curve with this formulation is shown in Fig. 1.

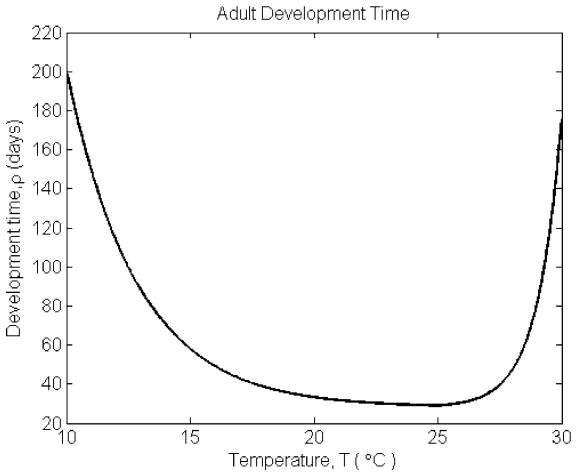

Fig. 1 An example of a development time curve. An insect's development time is the duration of a life stage at a certain temperature.

These curves are used to predict phenology for insects under variable temperatures. Define $T(t)$ to be the temperature at time t and $a(t)$ to be the proportion of a life stage that an insect has completed at that time, a dimensionless quantity taking values between 0 and 1. Since an insect takes $\rho_i(T)$ days to develop through the entire life stage at constant temperature T, the simplest developmental model predicts it will take $\Delta t = \rho_i(T)\Delta a$ days to develop through a fraction Δa of the life stage at that temperature. If the relationship $\Delta a/\Delta t = 1/\rho_i(T)$ holds for arbitrarily small values of Δt, i.e., $da/dt = 1/\rho_i(T(t))$, then development through stage i for an insect that began at time t_0 is described by the initial value problem

$$\frac{da}{dt} = \frac{1}{\rho_i(t)}, \qquad a(t_0) = 0, \tag{2}$$

where $\rho_i(t) = \rho_i(T(t))$. The differential equation (2) is integrated to determine the insect's age at time t,

$$a(t) = \int_{t_0}^{t} \frac{ds}{\rho_i(s)}.$$

In particular, the time that an insect will complete stage i if it began at time t, $g_i(t)$, satisfies

$$1 = \int_{t}^{g_i(t)} \frac{ds}{\rho_i(s)}. \tag{3}$$

When an insect completes a stage it begins the next stage; for example, an insect that enters stage 1 at time t will complete that stage and enter stage 2 at time $g_1(t)$. The same insect will complete stage 2 at time $g_2(g_1(t)) = (g_2 \circ g_1)(t)$. If $G(t)$ is the time that an

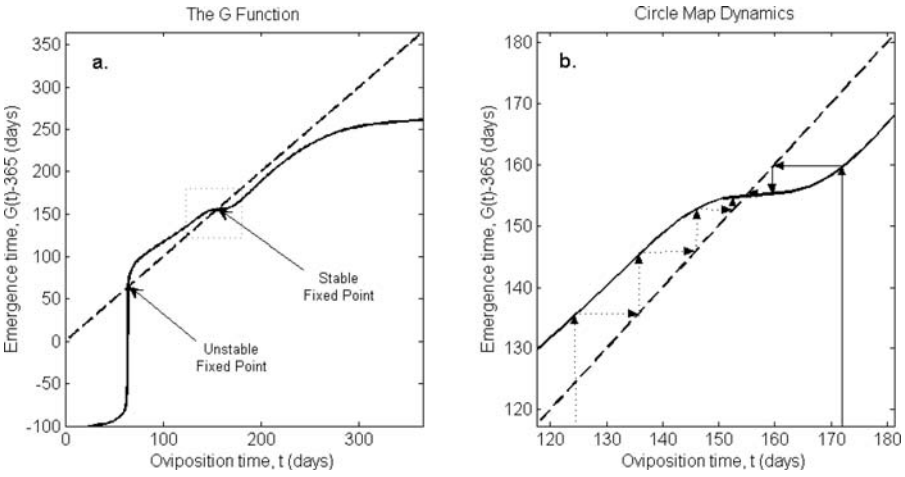

Fig. 2 (a) An example of a G function. Given the oviposition time t of an insect, its emergence time is $G(t)$. $G(t) - 365$ is plotted to show the time of year of emergence relative to the time of year of oviposition. (b) A developmental circle map and its fixed point dynamics. The circle map is the solid curve, and the fixed point line $G(t_o^n) = t_o^n$ is dashed. As the map is iterated oviposition time converges (arrows) to stable fixed points that occur at intersections of the two curves intersect where the slope of the circle map curve is less than one.

insect completes its life cycle when it began at time t, then for an insect with an m-stage life cycle

$$G(t) = (g_m \circ g_{m-1} \circ \cdots \circ g_2 \circ g_1)(t); \tag{4}$$

a typical G function is shown in Fig. 2.

Previous work has focused on the G function to understand the plastic response of phenology to temperature (Logan and Powell, 2001; Powell and Logan, 2005). If temperatures are periodic with the same variation each year (which is roughly true in natural systems), then the G function viewed modulo 365 days results in a periodic circle map between t_o^n, the time of year that an individual in generation n is oviposited, and t_o^{n+1}, the time of year that its offspring are oviposited in generation $n + 1$. Univoltine (one generation per year) fixed points of the circle map are times of year at which the oviposition times of an insect and its offspring are separated by exactly one year, i.e., $t_o^n = G(t_o^n) - 365$. These fixed points dominate the dynamics of the circle map when it is iterated over multiple generations (Powell and Logan, 2005), since oviposition times rapidly converge to these points regardless of initial oviposition time (see Fig. 2). Hence, univoltine fixed points can synchronize phenology within a population, and the timing of these fixed points relative to biotic and abiotic factors can have a profound effect on the average fitness of a population. The existence of fixed points is structurally stable; fixed points are maintained under small perturbations of development time curve parameters or the underlying temperature series (Powell and Logan, 2005). This stability plays an important role in the dynamics of our evolution model because individuals with slightly different phenotypes have slightly different G functions.

2.2. *Development time as a quantitative trait*

We model variation in development time by allowing a single developmental parameter, α, to vary continuously within a population. Let α scale some base development time curve $\rho_k(T)$ so that the development time in stage k for an individual with phenotype α is $\alpha\rho_k(T)$. Variance in α corresponds with realistic variance structure in development time; the same variation in α results in more variation at longer development times than at shorter development times as is often observed in development data. This means, for example, that an individual with phenotype $\alpha = 2$ takes twice as long to develop as an individual with phenotype $\alpha = 1$ at the same constant temperature. Variation in α may be linked to variation in insect size at maturity. The extension of our phenology model to account for α is straightforward: the time that an insect with phenotype α completes stage k given that it began at time t, $g_{k,\alpha}(t)$, satisfies

$$1 = \int_t^{g_{k,\alpha}(t)} \frac{ds}{\alpha\rho_k(s)},$$

similar to (3). For illustration purposes, we let development time vary within a single life stage. In this case, the emergence time of an individual with phenotype α that was oviposited at time t (its G function (4)), is

$$G_\alpha(t) = (g_m \circ g_{m-1} \circ \cdots \circ g_{k+1} \circ g_{k,\alpha} \circ g_{k-1} \circ \cdots \circ g_2 \circ g_1)(t).$$

Figure 3 shows examples of $G_\alpha(t)$ for various values of α.

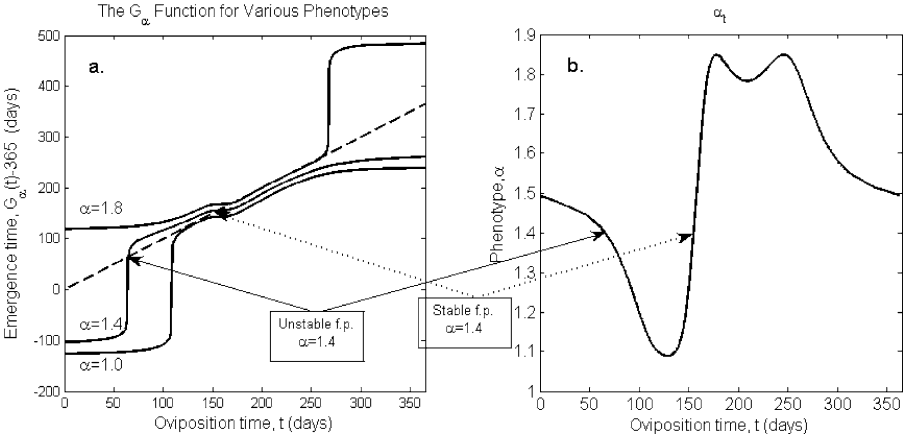

Fig. 3 (a) The G_α function for various values of α. Given the oviposition time t of an individual with phenotype α, the individual's emergence time is $G_\alpha(t)$. Although α varies continuously within a population, this plot shows only a few representative curves. (b) Given an oviposition time t, α_t is the unique phenotype that results in a univoltine fixed point for the G_α function at time t, i.e., $G_{\alpha_t}(t) = t + 365$. These fixed points are stable ($\frac{\partial}{\partial t}[G_{\alpha_t}(t)] < 1$) where α_t is increasing and unstable where α_t is decreasing (see text). The arrows point to the same unstable (solid) and stable (dotted) univoltine fixed points in both parts of the figure for individuals with phenotype $\alpha = 1.4$.

Under periodic temperatures, $G_\alpha(t)$ taken modulo 365 provides a circle map for each value of α, and this map may have univoltine fixed points. Conversely, given an oviposition time t there may be a phenotype, α_t, that results in a univoltine fixed point at time t, i.e., $t = G_{\alpha_t}(t) - 365$, (see Fig. 3). If we differentiate the definition of α_t with respect to t, upon rearrangement,

$$\dot{\alpha}_t = \frac{1 - \frac{\partial}{\partial t}[G_\alpha(t)]|_{\alpha=\alpha_t}}{\frac{\partial}{\partial \alpha}[G_\alpha(t)]|_{\alpha=\alpha_t}},$$

where '$\cdot$' indicates differentiation with respect to t. Increasing α increases development time, so the denominator is positive. If t is a stable fixed point of G_{α_t}, then $\frac{\partial}{\partial t}[G_\alpha(t)]|_{\alpha=\alpha_t} < 1$, so that the numerator is also positive, making $\dot{\alpha}_t > 0$. Similarly, $\dot{\alpha}_t < 0$ whenever t is a unstable fixed point of G_{α_t}. Stability of the univoltine fixed points in Fig. 3 can therefore be determined by the slope of α_t. Univoltine fixed points play a crucial role in organizing the dynamics of development within a population with developmental variability, since oviposition times are attracted to stable fixed points and repelled by unstable fixed points.

2.3. *Evolution map*

In this section, we describe how the phenotype-dependent phenology model is incorporated into a model of the evolution of phenology within a population. Let $p_o^n(\alpha, t)$ be the density of insects in generation n with phenotype α and oviposition time t; the evolution model maps $p_o^n(\alpha, t)$ to $p_o^{n+1}(\alpha, t)$. If selection acts only on emergence time and emergence density, then there are no selective pressures acting on the population during development, and the evolution map can be broken into two components: development and selection/reproduction (see Fig. 4). Development maps the oviposition distribution for generation n to the emergence distribution for generation n, i.e., $p_o^n(\alpha, t) \xrightarrow{D} p_e^n(\alpha, t)$. Selection and reproduction occur when the population emerges, mapping the emergence density for generation n to the oviposition distribution for generation $n + 1$, i.e., $p_e^n(\alpha, t) \xrightarrow{S,R} p_o^{n+1}(\alpha, t)$.

Now we derive an explicit representation for the development map in terms of the phenology model, leaving discussion of the selection and reproduction maps for Sections 2.4–2.5. If the number of insects is conserved during development (no mortality

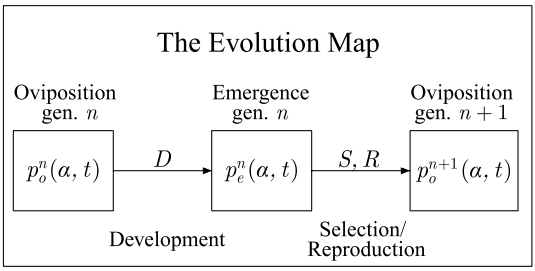

Fig. 4 A diagram of the evolution map. Development (D) maps the oviposition distribution to the emergence distribution for generation n. Selection/reproduction (S, R) maps the emergence distribution for generation n to the oviposition distribution for generation $n + 1$.

or immigration), then insects emerging between times t_1 and t_2 were oviposited between times $G_\alpha^{-1}(t_1)$ and $G_\alpha^{-1}(t_2)$;

$$\int_{t_1}^{t_2} p_e^n(\alpha, t)\, dt = \int_{G_\alpha^{-1}(t_2)}^{G_\alpha^{-1}(t_2)} p_o^n(\alpha, t)\, dt. \tag{5}$$

Changing variables results in

$$\int_{t_1}^{t_2} p_e^n(\alpha, t)\, dt = \int_{t_1}^{t_2} p_o^n\big(\alpha, G_\alpha^{-1}(t)\big) \frac{\partial}{\partial t}\big[G_\alpha^{-1}(t)\big]\, dt.$$

Since this equation must hold for all choices of t_1 and t_2, it follows that

$$p_e^n(\alpha, t) = p_o^n\big(\alpha, G_\alpha^{-1}(\alpha, t)\big) \frac{\partial}{\partial t}\big[G_\alpha^{-1}(\alpha, t)\big]. \tag{6}$$

Both forms of the conservation law ((5) and (6)) explicitly define the development map.

2.4. Natural selection

We discuss natural selection on emergence time and emergence density. In both cases, selection affects phenotypic variation indirectly, because insects with the same emergence time have the same fitness regardless of phenotype. In the first selection model, truncation selection acts on emergence time. If $S_1(t)$ is the fitness of individuals emerging at time t (the number of female eggs per female adult), then

$$S_1(t) = \begin{cases} \gamma_1, & t \in [t_{\text{early}}, t_{\text{late}}), \\ 0, & \text{otherwise.} \end{cases} \tag{7}$$

This selection function models the need for some insect species to emerge within a certain time interval to coincide with resource availability or to avoid lethal temperatures. We require that $365 \le t_{\text{early}} < t_{\text{late}} \le 730$, which confines cohorts to emerging within a single calendar year (univoltinism). Univoltinism is often necessary for a population to maintain adaptive seasonality (Logan and Powell, 2001).

In the second selection model, the fitness of an emerging individual depends on its emergence time and the density of simultaneous emergers. The emergence density at time t in generation n is

$$N_e^n(t) = \int p_e^n(\alpha, t)\, d\alpha. \tag{8}$$

The fitness of individuals emerging at time t, $S_2(t)$, has the following form:

$$S_2(t) = \begin{cases} F(N_e^n(t)), & t \in [t_{\text{early}}, t_{\text{late}}), \\ 0, & \text{otherwise,} \end{cases} \tag{9}$$

where F describes how fitness depends on emergence density. Here,

$$F(N) = \frac{\gamma_2 N}{N^2 + b^2}, \tag{10}$$

where γ_2 and b are positive parameters. $F(N)$ increases for $N < b$ and decreases for $N > b$, giving an Allee effect, since fitness increases with emergence density at low densities. F also accounts saturation at high densities ($F(N) \to 0$ as $N \to \infty$).

2.5. *Sexual reproduction*

Whereas the selection model determines the number of offspring produced per emerging female, the reproduction model determines their phenotypes. For simplicity, we assume that mating occurs immediately following emergence and results in the immediate production of $S(t)$ female eggs per female emerging at time t. Hence, mating only occurs between insects that emerge simultaneously, and the densities of parents and their offspring are related by

$$N_o^{n+1}(t) = S(t)N_e^n(t), \tag{11}$$

where $N_o^{n+1}(t)$ is the density of eggs oviposited at time t. We assume that the phenotypes of eggs laid at time t are normally distributed, so that the oviposition distribution in generation n is given by

$$p_o^n(\alpha, t) = \frac{N_o^n(t)}{\sqrt{2\pi v_o^n(t)}} \exp\left[\frac{-(\alpha - \mu_o^n(t))^2}{2v_o^n(t)}\right], \tag{12}$$

where $\mu_o^n(t)$ and $v_o^n(t)$ are the mean phenotype and phenotypic variance for the eggs laid at time t. The assumption of phenotypic normality is common in the quantitative genetic literature (e.g., Kimura, 1965; Lande, 1975; Slatkin, 1979). By using a normal distribution of phenotypes, we introduce negative and unbounded phenotypes into the population, but this effect is negligible if the mean phenotype is sufficiently large relative to the phenotypic variance.

We assume that progeny inherit their mean parent phenotype plus some error with zero mean and fixed variance σ_ε^2. This is similar to the approach introduced by Slatkin (1970). The reproductive variance is assumed to be small ($\sigma_\varepsilon^2 \ll 1$) and accounts for heterozygosity (Slatkin, 1970), maternal effects, environmental variability, and mutation. The phenotypes of females and males emerging simultaneously can be thought of as random variables F and M. Then the phenotype of their eggs is also a random variable, O, and

$$O = \frac{F}{2} + \frac{M}{2} + \varepsilon,$$

where ε is the reproductive error. If F and M are identically and independently distributed, with mean μ_e and variance v_e, then O has mean $\mu_o = \mu_e$, due to linearity of the mean, and variance $v_o = v_e/2 + \sigma_\varepsilon^2$, due to bilinearity of the covariance. Since most phenotypic variance can be attributed to reproductive variance (Slatkin, 1970), we rescale the phenotypic variance to obtain the order 1 quantity $v_e = \lambda v_e$, where $\lambda = 1/\sigma_\varepsilon^2$. Hence, if the mean phenotype and rescaled phenotypic variance of parents emerging at time t in generation n are $\mu_e^n(t)$ and $v_e^n(t)$, then the mean phenotype and rescaled phenotypic variance of their offspring are

$$\mu_o^{n+1}(t) = \mu_e^n(t), \tag{13}$$

$$v_o^{n+1}(t) = v_e^n(t)/2 + 1. \tag{14}$$

2.6. *Characterization of the evolution map*

The normality assumption (12) and the relationships between the densities (11), mean phenotypes (13), and rescaled phenotypic variances (14) of parents and offspring define the selection/reproduction component of the evolution model, mapping the emergence distribution for generation n to the oviposition distribution for generation $n+1$. Hence, the evolution map (e.g., Fig. 4) is characterized by these relationships and how development maps the density, mean phenotype, and rescaled phenotypic variance from oviposition to emergence:

$$\left\{N_o^n(t), \mu_o^n(t), v_o^n(t)\right\} \xrightarrow{D} \left\{N_e^n(t), \mu_e^n(t), v_e^n(t)\right\} \xrightarrow{S,R} \left\{N_o^{n+1}(t), \mu_o^{n+1}(t), v_o^{n+1}(t)\right\}.$$

In the remainder of this section, we provide the details of this characterization. The oviposition distribution for generation n (12) is

$$p_o^n(\alpha,t) = \sqrt{\frac{\lambda}{2\pi}}\left(\frac{N_o^n(t)}{\sqrt{v_o^n(t)}}\right)\exp\left[-\lambda\frac{(\alpha-\mu_o^n(t))^2}{2v_o^n(t)}\right]. \tag{15}$$

Following development (6), the emergence distribution for generation n is

$$p_e^n(\alpha,t) = \sqrt{\frac{\lambda}{2\pi}}\left(\frac{N_o^n(G_\alpha^{-1}(t))\frac{\partial}{\partial t}[G_\alpha^{-1}(t)]}{\sqrt{v_o^n(G_\alpha^{-1}(t))}}\right)\exp\left[-\lambda\frac{(\alpha-\mu_o^n(G_\alpha^{-1}(t)))^2}{2v_o^n(G_\alpha^{-1}(t))}\right]. \tag{16}$$

For notational simplicity, we define the following functions of α:

$$f_t(\alpha) = \frac{N_o^n(G_\alpha^{-1}(t))\frac{\partial}{\partial t}[G_\alpha^{-1}(t)]}{\sqrt{v_o^n(G_\alpha^{-1}(t))}}, \tag{17}$$

and

$$h_t(\alpha) = \frac{(\alpha-\mu_o^n(G_\alpha^{-1}(t))^2}{2v_o^n(G_\alpha^{-1}(t))}. \tag{18}$$

Then the emergence distribution (16) is given by

$$p_e^n(\alpha,t) = \sqrt{\frac{\lambda}{2\pi}}f_t(\alpha)\exp\left[-\lambda h_t(\alpha)\right].$$

The development map is characterized by the following integrals that give the density of individuals in generation n emerging at time t, their mean phenotype, and their rescaled phenotypic variance:

$$N_e^n(t) = \sqrt{\frac{\lambda}{2\pi}}\int_{-\infty}^{\infty} f_t(\alpha)\exp\left[-\lambda h_t(\alpha)\right]d\alpha, \tag{19}$$

$$\mu_e^n(t) = \frac{\sqrt{\lambda}}{N_e^n(t)\sqrt{2\pi}}\int_{-\infty}^{\infty}\alpha f_t(\alpha)\exp\left[-\lambda h_t(\alpha)\right]d\alpha, \tag{20}$$

$$v_e^n(t) = \frac{1}{N_e^n(t)\sqrt{2\pi\lambda}}\int_{-\infty}^{\infty}\left(\alpha-\mu_e^n(t)\right)^2 f_t(\alpha)\exp\left[-\lambda h_t(\alpha)\right]d\alpha. \tag{21}$$

Following development, the selection/reproduction map is applied giving,

$$N_o^{n+1}(t) = S(t)N_e^n(t),$$
$$\mu_o^{n+1}(t) = \mu_e^n(t),$$
$$v_o^{n+1}(t) = v_e^n(t)/2 + 1.$$

The preceding six equations completely characterize the evolution map.

3. Analytical results

We use Laplace's method (a special case of the method of steepest descent) to approximate each of the integrals defining the development map (19)–(21) by the leading order term of its asymptotic expansion as $\lambda \to \infty$ (see Bleistein and Handelsman, 1986; de Bruijn, 1981 for a discussion of the method). The results are used in Section 3.2.1 to approximate steady distributions in which the temporal structure of the mean phenotype and phenotypic variance are invariant under the evolution map with periodic temperatures. These steady distributions represent populations that are well adapted to stable climate conditions and are important in understanding the dynamics of the evolution model in general.

3.1. Approximation of the development map

3.1.1. Asymptotic expansions of development integrals

Applying Laplace's method to (19) results in the asymptotic expansion

$$N_e^n(t) = \frac{f_t(\alpha_t^\star)\exp[-\lambda h_t(\alpha_t^\star)]}{\sqrt{h_t''(\alpha_t^\star)}} + O\left(\frac{\exp[-\lambda h_t(\alpha_t^\star)]}{\lambda}\right),$$

as $\lambda \to \infty$, where $\alpha_t^\star$ is the value at which $h_t(\alpha)$ achieves a (in this case unique) minimum. Using an asymptotic expansion as $\lambda \to \infty$ is reasonable if the reproductive variance is small (i.e., $\sigma_\varepsilon^2 \ll 1$), since $\lambda = 1/\sigma_\varepsilon^2$. Truncating after the first term results in an approximation for the emergence density,

$$N_e^n(t) \approx \frac{f_t(\alpha_t^\star)\exp[-\lambda h_t(\alpha_t^\star)]}{\sqrt{h_t''(\alpha_t^\star)}}. \tag{22}$$

A similar approach gives the asymptotic expansion for the mean phenotype (20)

$$\mu_e^n(t) = \alpha_t^\star + O\left(\frac{1}{\lambda}\right),$$

as $\lambda \to \infty$, provided that $f_t(\alpha_t^\star) \neq 0$. The leading order term gives an approximation for the mean phenotype at emergence,

$$\mu_e^n(t) \approx \alpha_t^\star. \tag{23}$$

For the rescaled phenotypic variance, we must use a higher order expansion (see de Bruijn, 1981), since the first two terms in the asymptotic expansion for (21) are zero. Consequently,

$$v_e^n(t) = \frac{1}{h_t''(\alpha_t^\star)} + O\left(\frac{1}{\lambda}\right).$$

Truncating after the first term gives

$$v_e^n(t) \approx \frac{1}{h_t''(\alpha_t^\star)}. \tag{24}$$

3.1.2. Critical points of $h_t(\alpha)$

To find $\alpha_t^\star$ that minimizes $h_t(\alpha)$, we seek $\alpha_t^\star$ such that $h_t'(\alpha_t^\star) = 0$ and $h_t''(\alpha_t^\star) > 0$, where primes denote derivatives with respect to α. First, note that

$$\begin{aligned} h_t'(\alpha) = \frac{\alpha - \mu_o^n(G_\alpha^{-1}(t))}{2[v^n(G_\alpha^{-1}(t))]^2}\Bigg(&2v^n\big(G_\alpha^{-1}(t)\big)\Big(1 - \dot{\mu}_o^n\big(G_\alpha^{-1}(t)\big)\frac{\partial}{\partial\alpha}\big[G_\alpha^{-1}(t)\big]\Big) \\ &- \big(\alpha - \mu_o^n\big(G_\alpha^{-1}(t)\big)\big)\dot{v}^n\big(G_\alpha^{-1}(t)\big)\frac{\partial}{\partial\alpha}\big[G_\alpha^{-1}(t)\big]\Bigg), \end{aligned} \tag{25}$$

where '$\cdot$' denotes a derivative in time. In order for $\alpha_t^\star$ to be a critical point of $h_t(\alpha)$, either factor in (25) must be zero when $\alpha = \alpha_t^\star$. Setting the first factor in (25) equal to zero gives

$$\alpha_t^\star - \mu_o^n\big(G_{\alpha_t^\star}^{-1}(t)\big) = 0. \tag{26}$$

Setting the second factor in (25) equal to zero gives

$$\begin{aligned} 0 = 2v^n\big(G_{\alpha_t^\star}^{-1}(t)\big)&\Bigg(1 - \dot{\mu}_o^n\big(G_{\alpha_t^\star}^{-1}(t)\big)\frac{\partial}{\partial\alpha}\big[G_\alpha^{-1}(t)\big]\Big|_{\alpha=\alpha_t^\star}\Bigg) \\ &- \big(\alpha_t^\star - \mu_o^n\big(G_{\alpha_t^\star}^{-1}(t)\big)\big)\dot{v}^n\big(G_{\alpha_t^\star}^{-1}(t)\big)\frac{\partial}{\partial\alpha}\big[G_\alpha^{-1}(t)\big]\Big|_{\alpha=\alpha_t^\star}. \end{aligned}$$

Here, we focus on the first case, in which $\alpha_t^\star = \mu_o^n(G_{\alpha_t^\star}^{-1}(t))$, since it is consistent with numerical steady distribution results and leads to the simplest analysis. In this case, we know that $h_t(\alpha)$ achieves a minimum at $\alpha_t^\star$, since

$$h_t''(\alpha_t^\star) = \frac{\big(1 - \dot{\mu}_o(G_{\alpha_t^\star}^{-1}(t))\frac{\partial}{\partial\alpha}[G_\alpha^{-1}(t)]|_{\alpha=\alpha_t^\star}\big)^2}{v(G_{\alpha_t^\star}(t))} > 0. \tag{27}$$

3.2. Steady distributions of the evolution map

Under stable conditions, we expect that a well-adapted population will achieve some level of equilibrium with the local climate. To find equilibrium states, we seek oviposition distributions with structure that is invariant under the evolution map with periodic yearly

temperatures. Nontrivial steady states of the evolution map under periodic yearly temperatures may not exist if selection acts directly on emergence time and not on emergence density. Instead, steady distributions are sought in which the phenotypes of eggs oviposited at a particular time of year are invariant under the evolution map. These distributions are characterized by invariance of the mean phenotype and rescaled phenotypic variance, i.e.,

$$\mu_o^{n+1}(t+365) = \mu_o^n(t), \tag{28}$$

$$v_o^{n+1}(t+365) = v_o^n(t). \tag{29}$$

These conditions can be rewritten exclusively in terms of the development map since $\mu_o^{n+1}(t+365)$ and $v_o^{n+1}(t+365)$ are given in terms of $\mu_e^n(t+365)$ and $v_e^n(t+365)$ by the reproductive map (13)–(14). The results are the following conditions for a steady distribution:

$$\mu_e^n(t+365) = \mu_o^n(t), \tag{30}$$

$$v_e^n(t+365) = 2v_o^n(t) - 2. \tag{31}$$

3.2.1. Approximate steady distributions

We use the approximations generated using Laplace's method to characterize steady distributions at leading order. In particular, we replace $\mu_e^n(t+365)$ and $v_e^n(t+365)$ in the steady distribution conditions (30)–(31) by their approximations (23)–(24), giving

$$\mu_o^n(t) = \alpha^\star_{t+365}, \tag{32}$$

$$2v_o^n(t) - 2 = \frac{1}{h_t''(\alpha^\star_{t+365})}. \tag{33}$$

Recall that $\alpha^\star_{t+365}$ minimizes $h_t(\alpha)$ if (26) is satisfied, i.e., if

$$\alpha^\star_{t+365} = \mu_o^n\big(G^{-1}_{\alpha^\star_{t+365}}(t+365)\big).$$

Substituting into (32) yields

$$\mu_o^n(t) = \mu_o^n\big(G^{-1}_{\mu_o^n(t)}(t+365)\big), \tag{34}$$

a sufficiency condition for the mean phenotype at a steady distribution.

Note that (34) is satisfied if $G^{-1}_{\mu_o^n(t)}(t+365) = t$, which occurs by definition if

$$\mu_o^n(t) = \alpha_t. \tag{35}$$

In this case, the mean phenotype at time t results in a univoltine fixed point of G_α. We expect such a steady distribution to be stable when t is a stable fixed point of G_α, because emergence times are attracted to these points.

A condition for $v_o^n(t)$ when $\mu_o^n(t) = \alpha_t$ can be derived by working directly with (33). However, it is more informative to assume that the mean has reached its steady state

$\mu_o^n(t) = \alpha_t$, and consider the evolution of $v_o^n(t)$. Given the periodicity of α_t and (27), the Laplace approximation for the rescaled variance (24) becomes

$$v_e^n(t) \approx \frac{v_o^n(t)}{\left(1 - \dot{\alpha}_t \frac{\partial}{\partial \alpha}[G_\alpha^{-1}(t)]|_{\alpha=\alpha_t}\right)^2}. \tag{36}$$

Taken together, these give an approximation for the rescaled phenotypic variance when $\mu_o^n(t) = \alpha_t$. The squared quantity in the denominator has a particularly simple representation. Differentiating $t = G_{\alpha_t}^{-1}(t)$ with respect to t gives

$$1 = \dot{\alpha}_t \frac{\partial}{\partial \alpha}\left[G_\alpha^{-1}(t)\right]\Big|_{\alpha=\alpha_t} + \frac{\partial}{\partial t}\left[G_\alpha^{-1}(t)\right]\Big|_{\alpha=\alpha_t}.$$

This implies that the denominator in (36) is $(\frac{\partial}{\partial t}[G_\alpha^{-1}(t)]|_{\alpha=\alpha_t})^2$, so that

$$v_e^n(t) \approx v_o^n(t)\left(\frac{\partial}{\partial t}\left[G_\alpha(t)\right]\Big|_{\alpha=\alpha_t}\right)^2, \tag{37}$$

using the fact that

$$\frac{\partial}{\partial t}\left[G_\alpha^{-1}(t)\right]\Big|_{\alpha=\alpha_t} = \left(\frac{\partial}{\partial t}\left[G_\alpha(t)\right]\Big|_{\alpha=\alpha_t}\right)^{-1}.$$

The effect of the reproduction map on the rescaled phenotypic variance is given by

$$v_o^{n+1}(t) = \frac{v_e^n(t)}{2} + 1.$$

Substituting the Laplace approximation (37) for $v_e^n(t)$ gives

$$v_o^{n+1}(t) \approx \frac{v_o^n(t)}{2}\left(\frac{\partial}{\partial t}\left[G_\alpha(t)\right]\Big|_{\alpha=\alpha_t}\right)^2 + 1.$$

Repeated application of the evolution map under periodic temperature conditions results in the following:

$$v_o^{n+m}(t) \approx v_o^n(t)\left[x(t)\right]^m + \left[x(t)\right]^{m-1} + \left[x(t)\right]^{m-2} + \cdots + x(t) + 1,$$

where

$$x(t) = \frac{1}{2}\left(\frac{\partial}{\partial t}\left[G_\alpha(t)\right]\Big|_{\alpha=\alpha_t}\right)^2.$$

Assuming that $x(t) < 1$, the first term on the right-hand side vanishes as $m \to \infty$. Hence,

$$\lim_{m\to\infty} v_o^{n+m}(t) \approx \sum_{m=0}^{\infty}\left[x(t)\right]^m.$$

This geometric series converges to the limit $\frac{1}{1-x(t)}$ for values of t where $x(t) < 1$. This gives us the following result:

$$\lim_{n\to\infty} v_o^n(t) = \frac{1}{1 - \frac{1}{2}\left(\frac{\partial}{\partial t}[G_\alpha(t)]|_{\alpha=\alpha_t}\right)^2},$$

for values of t where

$$\frac{\partial}{\partial t}\left[G_\alpha(t)\right]\Big|_{\alpha=\alpha_t} < \sqrt{2}. \tag{38}$$

A quick check shows that

$$v_o^n(t) = \frac{1}{1 - \frac{1}{2}\left(\frac{\partial}{\partial t}[G_\alpha(t)]|_{\alpha=\alpha_t}\right)^2}, \tag{39}$$

satisfies the steady state condition (33).

3.2.2. Oviposition density dynamics at a steady distribution

We investigate the dynamics of the oviposition density, $N_o^n(t)$, at a steady distribution where $\mu_o^n(t) = \alpha_t$. The Laplace approximation (22) for the oviposition density at this steady distribution becomes

$$N_e^n(t) \approx \frac{f_t(\alpha_t)}{\sqrt{h_t''(\alpha_t)}}, \tag{40}$$

where (17) gives

$$f_t(\alpha_t) = \frac{N_o^n(t)}{\sqrt{v_o^n(t)}\frac{\partial}{\partial t}[G_\alpha(t)]|_{\alpha=\alpha_t}}.$$

Substituting the expression for $h_t''(\alpha_t)$ from (37) into Eq. (40) results in

$$N_e^n(t + 365) \approx N_o^n(t).$$

This gives us the relationship between the oviposition densities for generations n and $n + 1$,

$$N_o^{n+1}(t + 365) = S(t + 365)N_o^n(t). \tag{41}$$

The resulting dynamics are remarkably simple, since development and reproduction can be ignored at a steady distribution where $\mu_o^n(t) = \alpha_t$. The oviposition density is determined by the time of year and the density at the same time of year in the preceding generation. In the case of density dependent selection (9), $N_o^{n+1}(t) = H(N_o^n(t))$, where $H(N) = NF(N)$. The result is a discrete dynamical system, with dynamics characterized by properties of the function $H(N)$. In particular, oviposition density dynamics are determined by fixed points of $H(N)$ and their stability.

3.2.3. Summary and implications of steady distribution results

The analytical results suggest that populations experiencing periodic temperatures may evolve to steady distributions at times that are stable fixed points of the G_α function. We expect the temporal structure of the mean phenotype to evolve toward stable univoltine fixed points G_α as these points attract nearby emergence times. Our results also predict the phenotypic variance at steady distributions. The oviposition densities at stable fixed points of G_α are described by a simple dynamical map, H, from the oviposition density in one generation to the oviposition density in the next that is determined only by the selection function. We are careful here to distinguish between the three different types of steady state behavior that are important in the dynamics of the evolution model: steady distributions of the evolution map where the mean phenotype and phenotypic variance at oviposition is maintained from one generation to the next, fixed points of G_α where oviposition times are the same for parents with phenotype α and their offspring, and fixed points of H where the oviposition density of progeny is the same as the emergence density of their parents.

Although the structure of a steady distribution at unstable fixed points of G_α is not examined analytically, we expect it will be largely determined by the phenotypes of individuals leaked from nearby stable fixed points. For example, individuals with large phenotypes will leak from late stable fixed points to unstable fixed points that are later in the year. Hence, large phenotypes will probably dominate at these unstable fixed points. Due to the repulsive effect of unstable fixed points of G_α on emergence times, we expect emergence densities to be lower than at stable fixed points.

4. Numerical simulations

We numerically simulated the evolution of phenology for a model insect with two life stages. The purpose of these simulations was twofold: to verify our analytical results and to provide examples of dynamics of the evolution model. However, we do not intend to present a comprehensive analysis here of all possible dynamics. Instead, we restrict our attention to two long-term periodic temperature experiments with different selection functions and one short-term warming experiment with shifting resource phenology. A detailed description of the numerical implementation of the evolution map is given in the Appendix.

4.1. Two-stage model insect

The two-stage (egg and adult) model insect used here was constructed to have qualitatively similar phenology to most insects with temperature-dependent development. Since a two-stage life cycle has similar developmental dynamics to life cycles with more than 2 stages (Powell et al., 2000), our results generalize to more complicated systems. The model insect has piecewise exponential development time curves (1) shown in Fig. 5 with parameters in Table 1. Realistic parameters were obtained by fitting development time data for two mountain pine beetle life stages (Bentz et al., 1991), then scaling the curves to allow the model insect to be univoltine. Genetic variation in development time occurs in the adult stage. The development time of an adult is obtained by scaling the base adult

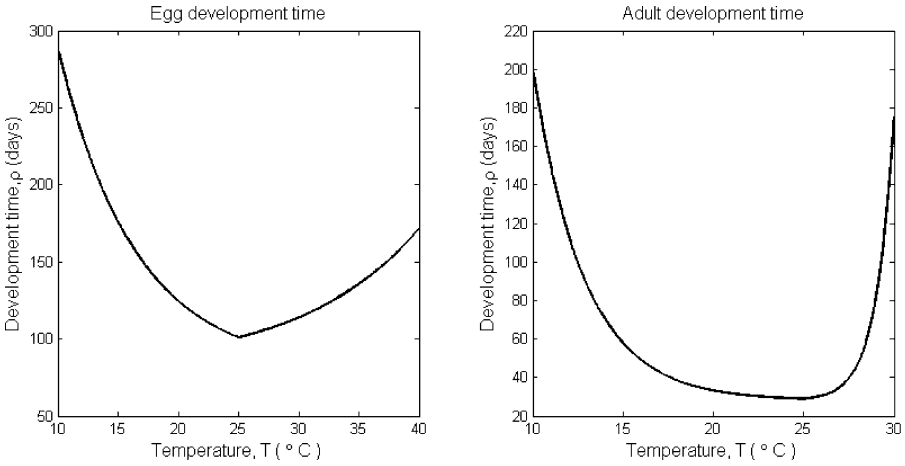

Fig. 5 Development time curves for the two-stage model insect. These curves are scaled mountain pine beetle development time curves.

Table 1 Development time curve parameters for 2-stage model insect used in numerical simulations

Stage	a	b	c	d	θ
Egg	81.000	6.899	0.156	0.101	25
Adult	28.036	8.658	0.351	1.022	25

development time curve by its phenotype, α. The reproductive variance for the model insects is set at $\sigma_\varepsilon^2 = 0.001$, which is consistent with developmental variation observed in mountain pine beetle populations.

4.2. Simulations: periodic temperature

To numerically investigate the structure of a population that is well adapted to stable climate conditions and to test our analytical steady distribution approximations, we performed two periodic temperature simulations with different selection functions. The periodic temperature series is a cosine curve such that the mean annual temperature is 8°C, the seasonal variation is 18°C, and the minimum temperature occurs on January 1, i.e., $T(t) = 8 - 18\cos(2\pi t/365)$. In both simulations, only insects emerging within a 100 day time window produce offspring (emergence time dependent truncation selection). In the first simulation, this is the only selection that occurs, so that selection is modeled by (7). In the second simulation, selection also depends on emergence density with an Allee effect according to (9)–(10). Selection parameters for both periodic temperature experiments are listed in Table 2. In the first simulation, we normalize the oviposition distribution at the beginning of each generation, because there is no density dependence to restrict population growth or decline. Given the parameter choices used in the second simulation (see Table 2), the emergence densities $N = 0$ and $N = 40{,}000$ are stable fixed points of $H(N)$, and $N = 10{,}000$ is an unstable fixed point of $H(N) = NF(N)$. Hence, when emergence

Table 2 Parameters for the selection functions in the periodic temperature simulations. In simulation 1, there is emergence time dependent truncation selection. In simulation 2, there is emergence time dependent truncation selection and density dependent selection with an Allee effect. The values listed for t_{early} and t_{late} are for generation n

Simulation	Parameter	Value
1 & 2	t_{early}	$365n + 100$
1 & 2	t_{late}	$365n + 200$
1	γ_1	1
2	γ_2	50,000
2	b	20,000

density drops below 10,000 the next generation's oviposition density declines, and when emergence density is above 10,000 the next generation's oviposition density is attracted to 40,000. The initial oviposition distributions are uniform over the phenotype-time rectangle $R = [0.8, 2.0] \times [0, 365]$, with $p_o^0(\alpha, t) = 10^5$ if $(\alpha, t) \in R$, and $p_o^0(\alpha, t) = 0$ otherwise. Simulations are run for 1,000 generations, after which $N_o^{1000}(t)$, $\mu_o^{1000}(t)$, and $v_o^{1000}(t)$ are computed for each time t and compared to the approximate steady distribution obtained by the Laplace method.

The results of the first periodic temperature simulation with no density dependent selection are shown in Fig. 6. After 1,000 generations, there is negligible change in the shape of the oviposition distribution in successive generations suggesting that a steady distribution is achieved. Most insects are oviposited at stable univoltine fixed points of G_α (see Fig. 6a). At these points, the mean phenotype closely follows the phenotype that allows a univoltine fixed point of the G_α function (see Fig. 6b). Hence, near stable fixed points the mean agrees with the steady distribution prediction that $\mu_o^n(t) \approx \alpha_t$. Furthermore, except near marginal (semistable) fixed points, the rescaled variance closely matches the corresponding steady distribution prediction (39) at stable fixed points of G_α (see Fig. 6c). At unstable fixed points, the numerical results do not match the steady distribution predictions. However, the oviposition density at these points is very low-the number of misbehaving insects is small relative to the total population.

The results of the second periodic temperature simulation with density-dependent selection are shown in Fig. 7. Similar to the first simulation, a steady distribution is reached within 1,000 generations and the validity of the steady distribution predictions depend on the stability of fixed points of G_α. At stable fixed points, the mean phenotype and rescaled phenotypic variance agree well with the phenotype that results in a univoltine fixed point and the corresponding prediction for the rescaled variance (see Fig. 7b–c). Near stable fixed points of G_α, the emergence density is reasonably close to the expected emergence density of 40,000 (see Fig. 7a). The emergence density declines at unstable fixed points but much less rapidly than in the first simulation, due to density dependent selection pushing it upward.

It is not surprising that the approximation $\mu_o^n(t) \approx \alpha_t$ fails near unstable fixed points at a steady distribution; the emergence times of individuals with phenotypes close to α_t are actually repelled by these points, so it is unlikely that the population could evolve toward them. The steady state approximations do allow us to understand the structure of steady distributions at unstable fixed points. Near marginal (semistable) fixed points individuals with certain phenotypes are leaked from stable to unstable fixed points. For example,

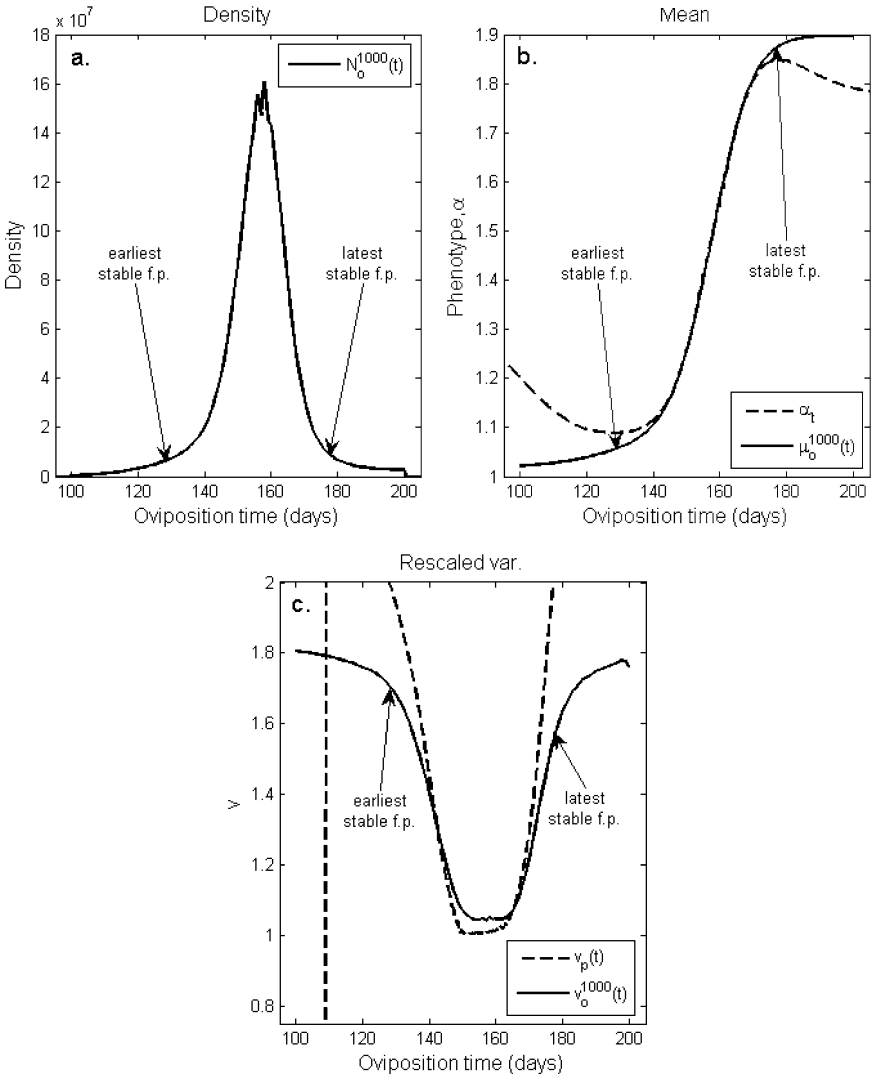

Fig. 6 Results after 1,000 generations of the first periodic temperature simulation with truncation selection on emergence time. The time of year of oviposition is shown on the horizontal axes. (a) Oviposition density. Most mass occurs at stable fixed points (between arrows). (b) Mean phenotype (solid) and α_t (dashed), the phenotype that makes t a univoltine fixed point of G_α. Consistent with analytical results, $\mu_o^n(t) \approx \alpha_t$ at stable fixed points. The prediction fails at unstable fixed points, where there is little mass and the population structure is mainly determined by the phenotypes of individuals leaked from nearby stable fixed points. (c) Rescaled phenotypic variance (solid) and $v_p(t)$ (dashed), the predicted rescaled variance at a steady distribution where $\mu_o^n(t) = \alpha_t$. Numerical rescaled variance results also agree with analytical predictions at all but the earliest and latest stable fixed points. The prediction does not hold at unstable fixed points where there is little mass.

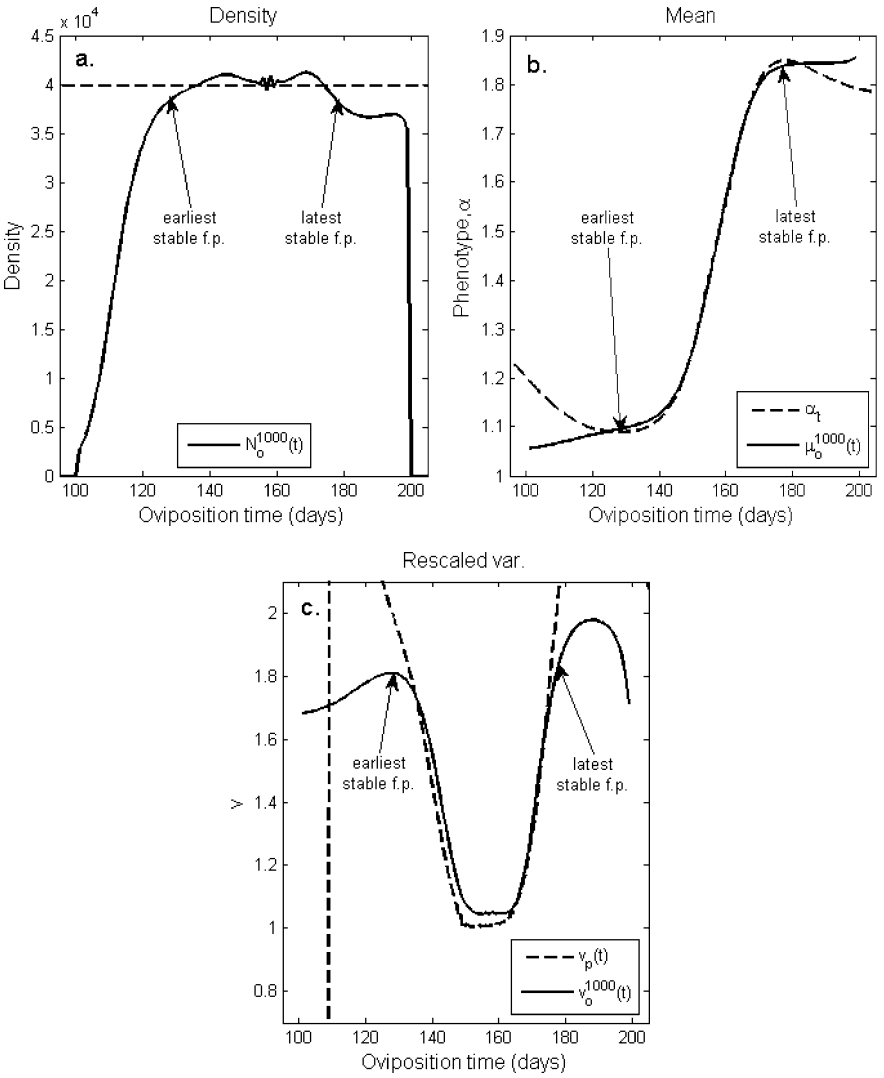

Fig. 7 Results after 1,000 generations of the second periodic temperature simulation with selection on emergence time and emergence density. The time of year of oviposition is shown on the horizontal axes. (a) Oviposition density (solid) and the predicted density (dash-dot) at a steady state where $\mu_o^n(t) = \alpha_t$ (40,000 is the nontrivial fixed point of $H(N)$). Most mass occurs at stable fixed points (between arrows). More mass is leaked to the unstable fixed points in this experiment than in the first periodic temperature experiment. This mass persists due to positive pressure from density dependent selection. (b) Mean phenotype (solid) and α_t (dashed), the phenotype that makes t a univoltine fixed point of G_α. Consistent with analytical results, $\mu_o^n(t) \approx \alpha_t$ at stable fixed points. The prediction fails at unstable fixed points, where the population structure is mainly determined by the phenotypes of individuals leaked from nearby stable fixed points. (c) Rescaled phenotypic variance (solid) and $v_p(t)$ (dashed), the predicted rescaled variance at a steady distribution where $\mu_o^n(t) = \alpha_t$. Numerical rescaled variance results also agree with analytical predictions at stable fixed points, but not at unstable fixed points.

individuals with large phenotypes oviposited at late stable fixed points will emerge later the next year on unstable fixed points. Hence, the phenotypes at unstable fixed points in a steady distribution are largely determined by the phenotypes of individuals leaking from nearby stable fixed points. This is apparent in Figs. 6b and 7b, where the phenotypes of individuals oviposited at times to the right (left) of the region of stable fixed points have larger (smaller) phenotypes than individuals oviposited at nearby marginal points. These results hold for a wide range of temperatures and parameters, except in the case where there are two or more disjoint regions of stable fixed points within the emergence time window. In this case, other numerical simulations show that the steady distribution approximation holds for the earliest region, but later regions tend to also be impacted by individuals leaked from the earlier stable fixed points. We expect that this discrepancy is due to the asymptotic nature of approximation, since as λ gets large reproductive variance gets small and there is less mixing between neighboring oviposition times. Hence, the approximation becomes worse as there is more mixing between regions of stable fixed points due to higher reproductive variance.

Our periodic temperature results suggest that variation in development time and phenology persist in a well-adapted population under stable climate conditions, both of these are observed in natural populations and in laboratory reared insects. Our analytical prediction that the mean phenotype at a steady distribution results in a univoltine fixed point of G_α agrees with numerical results at stable fixed points and is useful in understanding the population structure at nearby unstable fixed points. An interesting consequence of the structure of steady distributions is reproductive isolation of individuals with substantially different phenotypes. For example, individuals with large phenotypes emerge later than individuals with small phenotypes at a steady distribution causing their reproductive periods to be disjoint. This creates the potential for rapid local evolution if a disturbance during the emergence period removes early or late phenotypes.

4.3. Simulation: increasing temperature and advancing resource phenology

As an example of the dynamics of the evolution model under global warming, we simulated the evolution of a population of two-stage model insects with increasing mean annual temperature and advancing resource phenology (emergence window). The mean annual temperature is increased 6°C over 100 years by adding 6/100°C per year to the temperature series used in the preceding simulations: $T(t) = 8 - 18\cos(2\pi t/365) + (6/100)n$, where n is the number of calendar years that have passed at time t since the beginning of the simulation. This amount of warming is at the high end of current projections for some regions (Christensen et al., 2007), but the results generalize to less drastic scenarios. Selection depends on emergence time and density according to (9)–(10) with parameters in Table 3. The density dependence is the same as in the second periodic temperature experiment. In this simulation, individuals must emerge within a 20 day time window that advances 24 days over 100 years at a constant rate in order to reproduce, modeling changing resource phenology. This rate of phenology advance is similar to that observed in Memmott et al. (2007). The simulation begins with a population that is well-adapted to temperatures at the beginning of the experiment; the initial oviposition distribution is the from 1,000th generation in the second periodic temperature simulation. The increasing temperature simulation was run for 100 generations (100 years), and the number of insects oviposited in each generation, $\int_{365n}^{365(n+1)} N_o^n(t)\,dt$, was tracked.

Table 3 Parameters for the selection functions in the warming temperature simulations. There is truncation selection on emergence time with a shifting emergence window. There is also density dependent selection with an Allee effect. The values listed for t_{early} and t_{late} are for generation n

Parameter	Value
t_{early}	$515 + (365 - 24/100)n$
t_{late}	$535 + (365 - 24/100)n$
γ_2	50,000
b	20,000

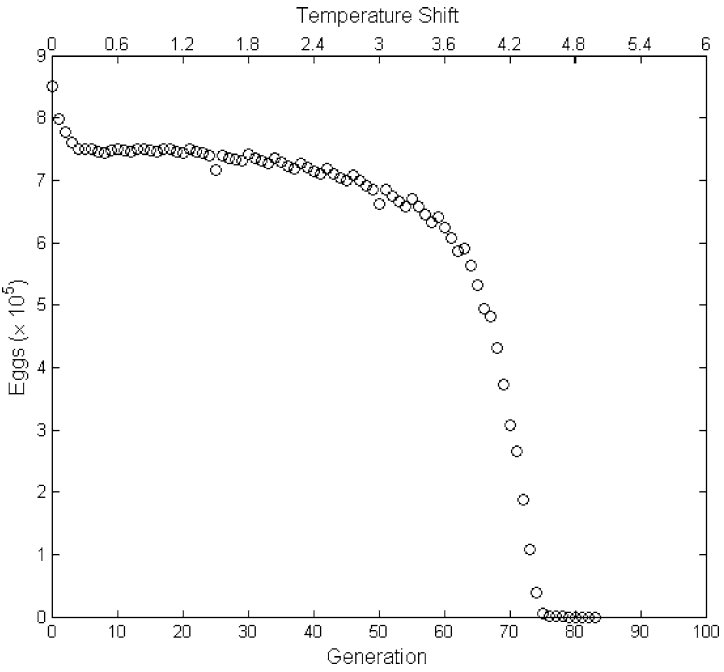

Fig. 8 Number of eggs laid per generation in the increasing temperature simulation. The generation number appears along the bottom horizontal axis, and the corresponding temperature shift appears along the top horizontal axis. In this simulation, mean annual temperature increases by 6°C over 100 years, and a 20 day long emergence window advances 24 days over 100 years. Density dependent selection is also imposed. The steep population decline between generations 60 and 73 corresponds to a loss of stable fixed points inside of the emergence time window.

The results of this simulation are shown in Fig. 8. The population declined slowly at first, but remained fairly large. After about 60 generations, the population dropped dramatically with zero insects remaining after 83 generations. The steep population decline coincides with a loss of stable fixed points within the shifting emergence time window (see Fig. 9). As temperatures increase, the time intervals over which G_α has stable fixed points change. The population evolves toward phenotypes that allow it to track changing stable fixed points as temperature increases, but when these fixed points do not overlap with the emergence time window the population rapidly declines. Outside of the region of

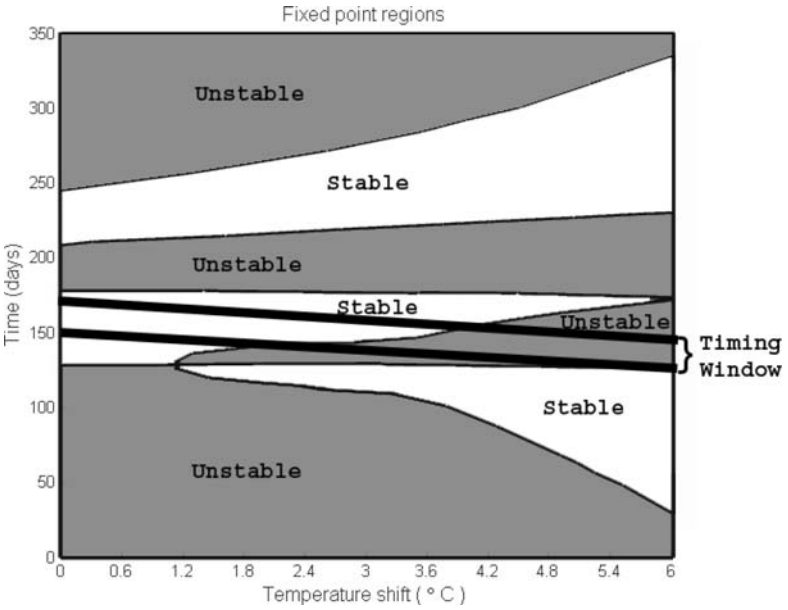

Fig. 9 A diagram of the stability of univoltine fixed points of the G_α function under different shifts of the temperature series $T(t) = 8 - 18\cos(2\pi t/365)$ and the emergence time window for the increasing temperature simulation (between thick black lines). For the two-stage model insect there is a phenotype α that makes each emergence time a univoltine fixed point of the G_α map. The stability of these fixed points is indicated in the diagram, with stable fixed points occurring in white regions and unstable fixed points occurring in gray regions. Note that after the temperature shift reaches 4.1°C there are no stable fixed points within the emergence time window. The loss of stable fixed points coincides with population collapse in the increasing temperature simulation.

stable fixed points individuals are pushed out of the emergence time window. The Allee affect keeps the population from rebounding if the system later evolves so the emergence time window overlaps with stable fixed points.

Our results show that genetic evolution may allow populations to persist for much longer than populations without evolution under global warming. To see this, we compare our results to the dynamics of a population with no developmental variation and no evolution of development time that experiences the same warming temperatures and shifting emergence window. Without evolution or variation of the plastic response of development time to temperature, populations can only remain viable if a stable fixed point of the G function is contained in the emergence time window. For example, if the entire population has phenotype $\alpha = 1.4$ and does not evolve, then the population will persist for approximately 20 generations under the temperature conditions in this simulation, since beyond this $G_{1.4}$ does not have a univoltine stable fixed point within the emergence window. This is much shorter than the evolving population persists (approximately 80 generations). Hence, our results show that evolution may allow a population to persist, but there is a limit; populations can only persist as long as the emergence time window overlaps with stable fixed points. Although we focus on a single scenario here, Fig. 9 can be used to predict population viability for the two-stage model insect under multiple scenarios of

climate warming and resource phenology shifts. Plotting the corresponding emergence window, the population is expected to decline rapidly as the window leaves regions of stable fixed points.

5. Summary and future directions

The evolution model presented here extends previous temperature-dependent phenology models by introducing heritable variation in their parameters. The model is presented in a general manner that is applicable to many insect species. Variation in development time is allowed to evolve in response to indirect selection acting on phenology instead of the development parameters themselves. The evolution map is characterized by its effects on the temporal variation of density, mean phenotype, and phenotypic variance at oviposition. We used this characterization and the Laplace method to approximate the evolution map and to identify important steady distributions where the mean phenotype allows for a univoltine fixed point of G_α.

Our analytical results suggest (and our numerical results verify) that populations that are well adapted to stable climate conditions are organized by stable univoltine fixed points of G_α. Populations rapidly adapt to track these points through evolution of the temporal structure of mean phenotype and phenotypic variance. The result is a population in which heritable variation in development time is maintained across successive generations. The stationary temporal structure of phenotypic variance at stable fixed points of G_α is determined by the slope of G_α. Steady distribution dynamics at unstable fixed points are largely determined by the population at neighboring stable fixed points, as individuals are leaked from stable to unstable fixed points depending on their phenotypes.

The numerical results also predict that populations may evolve to remain synchronized with resources as temperatures increase. However, this ability to adapt may disappear as overlap between stable univoltine fixed points of G_α and the timing of resource availability is lost. Unfortunately, this may cause sudden and otherwise unexpected local extinctions as observed in our numerical simulations.

The evolution dynamics presented here will provide a basis of comparison for future work in which more complex systems are analyzed. Our model is easily generalized by using different selection functions, phenology models, mating assumptions, or allowing different or multiple developmental parameters to vary. Variation in a scaling parameter results in variance in development time that is proportional to the square of mean development time. For simplicity, we ignored the effects of other types of developmental variance in this work. In the future, we will incorporate additional variance structures into a phenology model for mountain pine beetle using a Fokker–Planck equation (the phenology model without variation in development time presented here can be formulated as an advection equation). We will compare the evolution of phenology with additional random environmental noise to the analytical predictions presented here.

Acknowledgements

This work was supported by a Willard L. Eccles Foundation Graduate Fellowship and by the National Science Foundation under grant number DMS-0077663.

Appendix: Numerical methods

We describe the numerical methods that were used to implement the evolution model, including a detailed description of development and an overview of selection and reproduction. Fortunately, numerical solution of the evolution model does not require evaluation of the integrals in Eqs. (19)–(21). Instead, development of a population through each stage is treated separately and sequentially, followed by reproduction and selection.

In order to represent development through a life stage numerically, we first derive a conservation law governing the flow of insects from the beginning of a life stage to the end of the life stage. This conservation law is similar to the law derived for development through the entire life cycle (5). Let $p_i(\alpha, t)$ be the density of insects within the population with phenotype α that enter stage i at time t. We assume that there is no loss or gain of insects over the course of development though a stage (i.e., no mortality, immigration, or emigration during development), so insects that complete stage i (and enter stage $i+1$) between times t_1 and t_2 must have entered stage i between times $g_i^{-1}(t_1)$ and $g_i^{-1}(t_2)$. Then

$$\int_{t_1}^{t_2} p_{i+1}(\alpha, t)\, dt = \int_{g_i^{-1}(t_1)}^{g_i^{-1}(t_2)} p_i(\alpha, t)\, dt. \tag{A.1}$$

Note that if development time in stage i depends on the parameter α then g_i depends on α and (A.1) still holds.

Instead of tracking $p_i(\alpha, t)$ directly, we track integrals of $p_i(\alpha, t)$ over small time intervals (finite volumes) characteristics, i.e., from t to $g_i(t)$. Finite volume methods are conservative, so there is no loss of population density due to numerical error. The benefit of using a characteristic method is that development is tracked from the beginning of a stage to the end of the stage in one step. We define an equally-spaced time grid consisting of full-nodes, $\{1 = t_0, t_1, t_2, \ldots, t_w = 1095\}$, and an equally-spaced time grid consisting of half-nodes, $\{t_{-1/2}, t_{1/2}, t_{3/2}, t_{5/2}, \ldots, t_{w+1/2}\}$. In both cases, $t_y = 1 + y\Delta t$, where $\Delta t = 1094/(w-1)$. Let τ_j be the time interval $\tau_j = (t_{j-1/2}, t_{j+1/2}]$, noting that t_j is its midpoint. Tracking development over 3 years is more than sufficient, because in each simulation individuals that do not emerge during the second year are removed by truncation selection. In the α direction, the population is represented at regularly spaced grid points on a finite phenotype domain, $\{\alpha_1, \alpha_2, \ldots, \alpha_u\}$. Let $P_{j,k}^i$ be the number of insect with parameter α_k that enter stage i during the time interval τ_j:

$$P_{j,k}^i = \int_{t_{j-1/2}}^{t_{j+1/2}} p_i(\alpha_k, t)\, dt. \tag{A.2}$$

The conservation law (A.1) provides a map between $p_i(\alpha_k, t)$ and $P_{j,k}^{i+1}$,

$$\begin{aligned} P_{j,k}^{i+1} &= \int_{t_{j-1/2}}^{t_{j+1/2}} p_{i+1}(\alpha_k, t)\, dt, \\ &= \int_{g_i^{-1}(t_{j-1/2})}^{g_i^{-1}(t_{j+1/2})} p_i(\alpha_k, t)\, dt, \end{aligned}$$

$$= \int_{g_i^{-1}(t_{j-1/2})}^{t_{q-1/2}} p_i(\alpha_k, t)\, dt + \sum_{l=q+1}^{q+m-1} \left(\int_{t_{l-1/2}}^{t_{l+1/2}} p_i(\alpha_k, t)\, dt \right)$$
$$+ \int_{t_{q+m-1/2}}^{g_i^{-1}(t_{j+1/2})} p_i(\alpha_k, t)\, dt, \tag{A.3}$$

where $t_{q-1/2}$ through $t_{q+m-1/2}$ make up all of the half-nodes strictly between $g_i^{-1}(t_{j-1/2})$ and $g_i^{-1}(t_{j+1/2})$. The first and last integrals on the right-hand side of (A.3) are approximated, noting that $p_i(\alpha_k, t) \approx P_{j,k}^i/\Delta t$ for $t \epsilon \tau_j$. The other integrals in (A.3) are of the form in (A.2) so that

$$P_{j,k}^{i+1} \approx \left(\frac{t_{q-1/2} - g_i^{-1}(t_{j-1/2})}{\Delta t} \right) P_{q-1,k}^i$$
$$+ \sum_{l=q+1}^{q+m-1} P_{l,k}^i + \left(\frac{g_i^{-1}(t_{j+1/2}) - t_{q+m-1/2}}{\Delta t} \right) P_{q+m,k}^i. \tag{A.4}$$

This equation is used to find the number of insects that complete a stage during the time interval τ_j given information about insects entering the stage. We use Eq. (A.4) as the basis for our numerical method.

We compute $g_i^{-1}(t_{j-1/2})$ in (A.4) by first computing the number of age units accumulated between times $t_{-1/2}$ and $t_{j-1/2}$ for each half node (i.e., for $j = 1, 2, \ldots, w+1$). This cumulative age, A_j, is computed by numerically evaluating the integral

$$A_j = \int_{t_{-1/2}}^{t_{j-1/2}} \frac{ds}{\rho_i(s)},$$

noting that ρ_i and consequently A_j may depend on α. We find the first l such that $A_j - A_l \geq 1$, since then $g_i^{-1}(t_{j-1/2})$ is in the time interval τ_l and use linear interpolation to approximate $g_i^{-1}(t_{j-1/2})$.

Following development through each stage in the life cycle, selection, and reproduction are implemented. For the reproduction map, we compute the mean phenotype and phenotypic variance for individuals emerging over each time interval τ_j, as well as the number of individuals emerging over that interval. The next generation is initiated with an oviposition distribution in which the distribution of phenotypes of eggs laid during the time interval τ_j is Gaussian with the same mean phenotype as their parents and with phenotypic variance equal to half the parent phenotypic variance plus σ_ε^2. We scale this distribution so that the number of eggs laid over the interval τ_j is equal to the product of the number of parents that emerged over that interval and $S(t_j)$ for whichever selection function we are using.

References

Allee, W., Emerson, A., Park, O., Schmidt, K., 1949. Principles of Animal Ecology. Saunders, Philadelphia.

Bentz, B.J., Logan, J.A., Amman, G.D., 1991. Temperature-dependent development of the mountain pine beetle (Coleoptera: Scolytidae) and simulation of its phenology. Can. Entomol. 123, 1083–1094.
Bentz, B.J., Logan, J.A., Vandygriff, J., 2001. Latitudinal variation in *Dendroctonus ponderosae* (Coleoptera: Scolytidae) development time and adult size. Can. Entomol. 133, 375–387.
Berryman, A.A., Dennis, B., Raffa, K.F., Stenseth, N.C., 1985. Evolution of optimal group attack, with particular reference to bark beetles (Coleoptera: Scolytidae). Ecology 66(3), 898–903.
Bleistein, N., Handelsman, R.A., 1986. Asymptotic Expansion of Integrals. Dover, New York.
Calabrese, J.M., Fagan, W.F., 2004. Lost in time, lonely, and single: reproductive asynchrony and the Allee effect. Am. Nat. 164(1), 25–37.
Carroll, A., Taylor, S., Régnière, J., Safranyik, L., 2003. Effects of climate change on range expansion by the mountain pine beetle in British Columbia. In: Shore, T., Brooks, J., Stone, J. (Eds.), Mountain Pine Beetle Symposium: Challenges and Solutions. Information Report BC-X-399, pp. 223–232. Klowna, British Columbia, October 2003. Natural Resources Canada, Canadian Forest Service, Pacific Forestry Centre, Victoria.
Christensen, J.H., et al., 2007. Climate Change 2007: The Physical Science Basis. Contribution from Working Group I to the Fourth Assessment Report of the Intergovernmental Panel on Climate Change. Cambridge University Press, Cambridge.
Danks, H.V., 1987. Insect Dormancy: An Ecological Prospective. Monograph Series, vol. 1. Biological Survey of Canada (Terrestrial Arthropods), Ottawa.
de Bruijn, N.G., 1981. Asymptotic Methods in Analysis. Dover, New York.
Eubank, W., Atmar, J., Ellington, J., 1973. The significance and thermodynamics of fluctuating versus static thermal environments on *Helios zea egg development rates*. Environ. Entomol. 2(4), 491–496.
Gilbert, E., Powell, J.A., Logan, J.A., 2004. Comparison of three models predicting developmental milestones given environmental and individual variation. Bull. Math. Biol. 66, 1821–1850.
Hartl, D.L., 2000. A Primer of Population Genetics, 3rd edn. Sunderland, Massachusetts.
Jenkins, J.L., Powell, J.A., Logan, J.A., Bentz, B.J., 2001. Low seasonal temperatures promote life cycle synchronization. Bull. Math. Biol. 63(3), 573–595.
Johnoson, T., Barton, N., 2005. Theoretical models of selection and mutation on quantitative traits. Philos. Trans. R. Soc. B 360, 1411–1425.
Kimura, M., 1965. A stochastic model concerning the maintenance of genetic variability in quantitative characters. Proc. Natl. Acad. Sci. USA 54, 731–736.
Lande, R., 1975. The maintenance of genetic variability by mutation in a polygenic character with linked loci. Genet. Res. 26, 221–235.
Logan, J.A., Powell, J.A., 2001. Ghost forests, global warming and the mountain pine beetle. Am. Entomol. 47, 160–173.
Memmott, J., Craze, P.G., Waser, N.M., Price, M.V., 2007. Global warming and the disruption of plant-pollinator interactions. Ecol. Lett. 10, 710–717.
Parmesan, C., Yohe, G., 2003. A globally coherent fingerprint of climate change impacts across natural systems. Nature 421, 37–42.
Powell, J.A., Logan, J.A., 2005. Insect seasonality: circle map analysis of temperature-driven life cycles. Theor. Popul. Biol. 67, 161–179.
Powell, J.A., Jenkins, J.L., Logan, J.A., Bentz, B.J., 2000. Seasonal temperature alone can synchronize life cycles. Bull. Math. Biol. 62(5), 977–998.
Sharpe, P., DeMichele, D., 1977. Reaction kinetics of poikilotherm development. J. Theor. Biol. 64, 649–670.
Slatkin, M., 1970. Selection and polygenic characters. Proc. Natl. Acad. Sci. USA 66(1), 87–93.
Slatkin, M., 1979. Frequency- and density-dependent selection on a quantitative character. Genetics 93, 755–771.
Taylor, F., 1981. Ecology and the evolution of physiological time in insects. Am. Nat. 117(1), 1–23.
Visser, M.E., Holleman, L.J.M., 2001. Warmer springs disrupt the synchrony of oak and winter moth phenology. Proc. R. Soc. Lond. 268, 289–294.
Zaslavski, V., 1988. Insect Development: Photoperiodic and Temperature Control. Springer, Berlin.